only about 0.6 eV, but d function exclusion in the Cl 2p ← 1e transition-state calculations leads to a transition energy of 207.2 eV, more than 4 eV larger than the value of 202.9 eV obtained when d functions are included (Table II). Thus, the inclusion of d functions on the metal is also important in describing the electronic relaxation attendant upon core hole creation which is needed to obtain the correct transition energy.

In addition to the major effect of 3d-orbital participation upon the L XE intensities, small effects arising from other approximations were also observed. We find that orbital compositions and computed oscillator strengths are somewhat changed in going from the ground state of the oxyanion to the XE transition state. For ClO_4^- the Cl 3d character in the 1e orbital increases from 5.5 to 6.4% while the Cl 3s character in the $2a_1$ orbital drops from 16.8 to 14.9% and rises in the $1a_1$ orbital from 50.9 to 57.9. Since Cl-centered orbitals will be stabilized in the L XE transition state, the Cl 3d orbital is expected to be pulled down toward the O 2p, resulting in more Cl 3d–O 2p covalent mixing, while the Cl 3s is pulled further below the O 2s, reducing the Cl 3s–O 2s covalent mixing. Percentage changes in oscillator strengths between the ground and transition states closely match those in orbital population, as illustrated in Table IV. Thus, core hole creation seems to have only a modest effect upon intensities although it strongly modifies energies (e.g., the Cl 2p ← 1e orbital eigenvalue difference increases from 189.7 eV in the ground state to 202.9 eV in the transition state).

Allowance for delocalization of the "Cl 2p" orbital onto the oxygens in the XE transition state increases the intensity of the Cl 2p ← 1e transitions by about one-third but modifies the other transition intensities (including that to the $3t_2$ orbital) by only a few percent. This effect therefore has only a modest influence on the relative emission intensities from the 1e, $3t_2$, and $2a_1$ orbitals.

The remaining discrepancies between calculated and experimental relative intensities may arise from either the limitations of the SCF–Xα scattered-wave method and/or the neglect of the crystalline environment. Since the discrepancy is substantially larger for PO_4^{3-} than for ClO_4^-, the latter factor may be the more important. It is also probable that PO_4^{3-} would be a better model for an ionic phosphate like Na_3PO_4 than it is for $AlPO_4$, whose spectrum yielded the experimental intensities given in Table I.

Conclusion

The SCF–Xα method yields L XE energies and intensities in semiquantitative agreement with experiment for PO_4^{3-} and ClO_4^-. Qualitative trends in peak intensities may be predicted from an inspection of orbital compositions. However, quantitative calculation of the spectral intensities requires the consideration of different radial functions for central-atom 3s and 3d orbitals. In addition to its effect upon transition intensity, 3d-orbital participation is found to strongly modify transition energies.

Acknowledgment. The calculations reported here were supported partly by the Computer Science Center of the University of Maryland and partly by the National Science Foundation, Grant No. EAR 7801780. Dr. D. S. Urch provided valuable assistance in interpreting the perchlorate experimental data, and Dr. L. Noodleman provided help in testing and running the modified SCF–Xα program. Collaborative discussions of the spectra were supported by NATO, Grant No. 1509.

Registry No. PO_4^{3-}, 14265-44-2; ClO_4^-, 14797-73-0.

Contribution from the School of Chemical Sciences, University of Illinois, Urbana, Illinois 61801

Electron Transfer in Mixed-Valent Diferrocenylacetylene and [2.2]Ferrocenophane-1,13-diyne

JACK A. KRAMER and DAVID N. HENDRICKSON*[1]

Received March 17, 1980

The preparation and characterization of triiodide salts of mixed-valent and dioxidized diferrocenylacetylene and [2.2]-ferrocenophane-1,13-diyne are reported. Iron-57 Mössbauer data show that the mixed-valent salt of diferrocenylacetylene is localized, whereas the mixed-valent salt of [2.2]ferrocenophane-1,13-diyne is delocalized. The latter salt is also shown to be delocalized on the EPR time scale. A criterion based on the appearance of the perpendicular C–H bending bands in the infrared spectrum is developed to tell whether a given mixed-valent ferrocene is delocalized or not on the vibrational time scale. Results are given for mixed-valent salts of [2.21ferrocenophane-1,13-diyne, biferrocene, 1′-acetylbiferrocene, and bis(fulvalene)dicobalt(II,III)(1+). The dioxidized triiodide salt of diferrocenylacetylene is shown to exhibit an antiferromagnetic interaction where μ_{eff}/Fe decreases to 1.39 μ_B at 4.2 K. And finally, insight about the mixed-valent phenomenon in fused ferrocenes is gained by a correlation of **g**-tensor anisotropy with the magnitude of quadrupole splitting observed.

Introduction

In 1974, Cowan and co-workers reported[2] the electrochemical generation of the mixed-valence ion of a diferrocenylacetylene (I). They found that there is a 130-mV separation between the two one-electron half-wave oxidation potentials of I. The mixed-valence monocation of I has an intervalence transfer (IT) electronic absorption band at 6410 cm^{-1} (ϵ = 670). A later report[3] from the same workers showed that

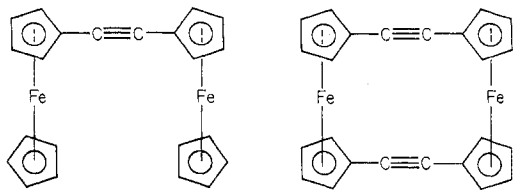

I II

[2.2]ferrocenophane-1,13-diyne (II) exhibits two reversible one-electron oxidation waves with a separation of 355 mV. A relatively intense (ϵ = 3100) IT band is seen at 5680 cm^{-1} for the mixed-valence monocation of II. The EPR spectrum of this same mixed-valence ion in a methylene chloride glass at

(1) A. P. Sloan Foundation Fellowship, 1976–1978.
(2) LeVanda, C.; Cowan, D. O.; Leitch, C.; Bechgaard, K. *J. Am. Chem. Soc.* **1974**, *96*, 6788.
(3) LeVanda, C.; Bechgaard, K.; Cowan, D. O. *J. Org. Chem.* **1976**, *41*, 2700.

0020-1669/80/1319-3330$01.00/0

Table I. Analytical Data

compd	%C calcd	%C obsd	%H calcd	%H obsd	%M calcd	%M obsd	%I calcd	%I obsd
$(\eta^5\text{-}C_5H_5)Fe(\eta^{10}\text{-}C_5H_4C{\equiv}CC_5H_4)Fe(\eta^5\text{-}C_5H_5)$	67.05	66.71	4.60	4.55	28.34	27.89		
$[(\eta^5\text{-}C_5H_5)Fe(\eta^{10}\text{-}C_5H_4C{\equiv}CC_5H_4)Fe(\eta^5\text{-}C_5H_5)](I_3)_2$	22.87	22.30	1.57	1.67	9.67	9.60	65.90	66.22
$[(\eta^5\text{-}C_5H_5)Fe(\eta^{10}\text{-}C_5H_4C{\equiv}CC_5H_4)Fe(\eta^5\text{-}C_5H_5)](BF_4)_2$	46.55	45.89	3.20	3.25	19.67	19.89		
$[Fe(\eta^{10}\text{-}C_5H_4C{\equiv}CC_5H_4)_2Fe](I_3)\cdot{}^3/_4I_2$	29.20	29.85	1.63	1.61	11.31	11.24	57.85	56.78
$[(\eta^5\text{-}C_5H_5)Fe(\eta^{10}\text{-}C_{10}H_8)Fe(\eta^5\text{-}C_5H_4)]I_3\cdot I_2$	23.96	24.07	1.61	1.62	11.14	11.07		
$(\eta^5\text{-}CH_3COC_5H_4)Fe(\eta^{10}\text{-}C_{10}H_8)Fe(\eta^5\text{-}C_5H_5)$	64.12	63.44	4.89	4.90	27.10	26.47		
$[(\eta^5\text{-}CH_3COC_5H_4)Fe(\eta^{10}\text{-}C_{10}H_8)Fe(\eta^5\text{-}C_5H_5)]I_3\cdot{}^1/_2I_2$	28.73	29.76	2.19	2.23	12.14	11.98		
$[Co(\eta^{10}\text{-}C_{10}H_8)_2Co](PF_6)_2$	46.26	46.38	3.11	3.40	22.60	22.22		
$[Co(\eta^{10}\text{-}C_{10}H_8)_2Co]PF_6$	36.16	36.31	2.44	2.67	17.75	16.87		
$[(\eta^5\text{-}CH_3COC_5H_4)Fe(\eta^5\text{-}C_5H_5)]I_5$	16.71	17.47	1.40	1.39	6.46	6.61		

Table II. Parameters Resultant from Least-Squares Fitting of ^{57}Fe Mössbauer Spectra[a]

compd	T, K	ΔE_Q	δ[b]	Γ[c]
$(\eta^5\text{-}C_5H_5)Fe(\eta^{10}\text{-}C_5H_4C{\equiv}CC_5H_4)Fe(\eta^5\text{-}C_5H_5)$[d]	78	2.41 (2)	0.50 (2)	
$[(\eta^5\text{-}C_5H_5)Fe(\eta^{10}\text{-}C_5H_4C{\equiv}CC_5H_4)Fe(\eta^5\text{-}C_5H_5)]I_3$[d]	78	2.18 (2), 0.49 (2)	0.54 (2), 0.50 (2)	
$[(\eta^5\text{-}C_5H_5)Fe(\eta^{10}\text{-}C_5H_4C{\equiv}CC_5H_4)Fe(\eta^5\text{-}C_5H_5)](I_3)_2$	77	0.222 (6)	0.506 (8)	0.538 (14), 0.368 (6)
$Fe(\eta^{10}\text{-}C_5H_4C{\equiv}CC_5H_4)_2Fe$[d]	78	2.41 (2)	0.56 (2)	
$[Fe(\eta^{10}\text{-}C_5H_4C{\equiv}CC_5H_4)_2Fe]I_3\cdot{}^3/_4I_2$	298	1.519 (5)	0.444 (7)	0.322 (10), 0.292 (8)
$[Fe(\eta^{10}\text{-}C_5H_4C{\equiv}CC_5H_4)_2Fe]I_3\cdot I_2$[d]	78	1.61 (2)	0.54 (2)	
$[(\eta^5\text{-}CH_3COC_5H_4)Fe(\eta^{10}\text{-}C_{10}H_8)Fe(\eta^5\text{-}C_5H_5)]I_3\cdot{}^1/_2I_2$	298	2.089 (13), 0.280 (18)	0.413 (15), 0.415 (21)	0.145 (13), 0.134 (12) 0.207 (20), 0.194 (18)
$[(\eta^5\text{-}CH_3COC_5H_4)Fe(\eta^5\text{-}C_5H_5)]I_3\cdot I_2$	298	0.233 (16)	0.408 (20)	0.198 (19), 0.151 (12)

[a] ΔE_Q, δ, and Γ values are in mm/s; the estimated error in the least-significant figure is given in parentheses. [b] Isomer shift relative to iron metal. [c] Full width at half-height taken from the Lorentzian fitting program. The width for the line at more negative velocity is listed first. [d] Reference 6.

77 K was found to be similar to the spectrum of the mixed-valence bis(fulvalene)diiron(1+) ion, which is known[4,5] to be a delocalized species. It was thus suggested that the mixed-valence monocation of II is also delocalized.

It was the goal of the work described in this paper to prepare salts of the mixed-valence ions of I and II and to use EPR, ^{57}Fe Mössbauer, and IR spectral data to characterize the rate of electron transfer in these interesting ions. During the course of this work, ^{57}Fe Mössbauer spectra were reported[6] for I, II, and the triiodide salts of the corresponding mixed-valence ions. These results will be used to confirm and supplement the data reported in the present paper.

Experimental Section

Physical Measurements. Infrared spectra were obtained with Perkin-Elmer Model 283 and Beckman Model IR-12 grating spectrophotometers. All samples were prepared as 13-mm KBr pellets with 2–5 mg of compound/100 mg of KBr.

Variable-temperature magnetic susceptibility measurements were made with a PAR Model 150A vibrating-sample magnetometer as previously described.[7] Corrections for background and sample diamagnetism[8] were made.

EPR spectra were obtained with a Varian E-9 X-band spectrometer equipped with a Varian temperature controller (80–350 K). Spectra obtained in the range of 2.8–20 K were recorded by employing an Oxford Instrument helium-flow cooling unit.

Iron-57 Mössbauer spectra were obtained with an instrument which has been described.[9] Computer fittings of the data to Lorentzian lines were carried out with a modified version of a previously reported program.[10] Isomer shifts are reported relative to iron metal.

Compound Preparation. Elemental analyses were performed by the Microanalytical Laboratory of the School of Chemical Sciences. Analytical data are given in Table I.

A sample of **diferrocenylacetylene** was prepared according to literature methods.[11,12] Diferrocenylacetylene was oxidized in benzene in a manner analogous to that used for biferrocene[4] to give the dioxidized salt $[(\eta^5\text{-}C_5H_5)Fe(\eta^{10}\text{-}C_5H_4C{\equiv}CC_5H_4)Fe(\eta^5\text{-}C_5H_5)](I_3)_2$. We also found that diferrocenylacetylene is dioxidized by *p*-benzoquinone and HBF_4 in ether to give a BF_4^- salt. Oxidation by sulfuric acid[4] resulted in decomposition of diferrocenylacetylene. In our hands, attempts to prepare a I_3^- salt of the mixed-valence monocation of diferrocenylacetylene by use of stoichiometric amounts of iodine resulted in a mixture of orange and black materials upon evaporation.

A sample of [2.2]ferrocenophane-1,13-diyne was prepared by literature methods.[13] It was found that an improved yield of 1-(chloromercuri)-1′-(2-formyl-1-chlorovinyl)ferrocene could be obtained by mixing the perchloric acid catalyst with the (2-formyl-1-chlorovinyl)ferrocene instead of adding it dropwise with the mercuric acetate solution. The sample of II was identified by its mass spectrum and then oxidized by iodine in benzene to give $[Fe(\eta^{10}\text{-}C_5H_4C{\equiv}CC_5H_4)_2Fe]I_3\cdot{}^3/_4I_2$.

A sample of the $I_3^-\cdot{}^1/_2I_2$ salt of **biferrocene** was prepared as reported.[4] **1′-Acetylbiferrocene** was prepared according to the literature method[14] and was characterized by a mass spectrum and by analysis. It was oxidized by iodine in benzene to give $[(\eta^5\text{-}CH_3COC_5H_4)Fe(\eta^{10}\text{-}C_{10}H_8)Fe(\eta^5\text{-}C_5H_5)]I_3\cdot{}^1/_2I_2$.

Samples of [bis(fulvalene)dicobalt]$(PF_6)_2$, i.e., $[Co(\eta^{10}\text{-}C_{10}H_8)_2Co](PF_6)_2$, and [bis(fulvalene)dicobalt]PF_6 were prepared by reported methods.[15,16]

Results and Discussion

Mössbauer Spectroscopy. Diferrocenylacetylene (I) and [2.2]ferrocenophane-1,13-diyne (II) were oxidized by I_2 in benzene to give the triiodide salts $[(\eta^5\text{-}C_5H_5)Fe(\eta^{10}\text{-}C_5H_4C{\equiv}CC_5H_4)Fe(\eta^5\text{-}C_5H_5)](I_3)_2$ and $[Fe(\eta^{10}\text{-}C_5H_4C{\equiv}CC_5H_4)_2Fe]I_3\cdot{}^3/_4I_2$, respectively. The stoichiometry of the first salt indicates that both iron ions are oxidized in the treatment of molecule I with I_2. A ^{57}Fe Mössbauer spectrum was run

(4) Morrison, W. H., Jr.; Hendrickson, D. N. *Inorg. Chem.* **1975**, *14*, 2331.
(5) LeVanda, C.; Bechgaard, K.; Cowan, D. O.; Mueller-Westerhoff, U. T.; Eilbracht, P.; Candela, G. A.; Collins, R. L. *J. Am. Chem. Soc.* **1976**, *98*, 3181.
(6) Motoyama, I.; Watanabe, M.; Sano, H. *Chem. Lett.* **1978**, 513.
(7) Francesconi, L. C.; Corbin, D. R.; Hendrickson, D. N.; Stucky, G. D. *Inorg. Chem.* **1979**, *18*, 3074.
(8) Figgis, B. N.; Lewis, J. *Mod. Coord. Chem.* **1960**, 403.
(9) Münck, E.; Debrunner, P. G.; Tsibris, J. C. M.; Gunsalus, I. C. *Biochemistry* **1972**, *11*, 855.
(10) Chrisman, B. L.; Tumolillo, T. A. *Comput. Phys. Commun.* **1971**, *2*, 322.
(11) Rosenblum, M.; Brown, N.; Papenmeier, J.; Applebaum, M. *J. Organomet. Chem.* **1966**, *6*, 173.
(12) Abram, T. S.; Watts, W. E. *Synth. React. Inorg. Met.-Org. Chem.* **1976**, *6*, 31.
(13) Rosenblum, M.; Brown, N. M.; Ciappenelli, D.; Tancrede, J., Jr. *J. Organomet. Chem.* **1970**, *24*, 469.
(14) Rausch, M. D. *J. Org. Chem.* **1964**, *29*, 1257.
(15) Davison, A.; Smart, J. C. *J. Organomet. Chem.* **1973**, *49*, C43.
(16) Smart, J. C. Ph.D. Thesis, Massachusetts Institute of Technology, 1974.

Table III. Corrected Paramagnetic Susceptibility Data for $[Fe(\eta^{10}\text{-}C_5H_4C{\equiv}CC_5H_4)_2Fe]I_3{\cdot}^3/_4I_2$

T, K	$10^3\chi_M$,[a] cgsu	μ_{eff},[b] μ_B	T, K	$10^3\chi_M$,[a] cgsu	μ_{eff},[b] μ_B
55.9	12.2	2.34	7.1	73.4	2.04
39.8	15.9	2.25	6.6	77.6	2.03
32.2	18.9	2.20	6.2	81.8	2.02
23.7	24.8	2.17	5.9	87.1	2.03
16.9	35.0	2.17	5.7	91.8	2.05
13.6	42.0	2.14	4.2	127.2	2.07

[a] Molar paramagnetic susceptibilities are corrected for background and compound diamagnetism, calculated from Pascal's constant to be -411.7 cgsu/mol. [b] Calculated with the assumption of one paramagnetic center per molecule.

at 80 K for the triiodide salt of diferrocenylacetylene and this spectrum substantiates the fact that the cation of I is dioxidized in this salt. One quadrupole-split doublet is present in the spectrum. Least-squares fitting the spectrum gives ΔE_Q = 0.222 (6) mm/s and δ = 0.506 (8) mm/s vs. iron metal (see Table II).

Motoyama et al.[6] were able to prepare an I_3^- salt of the mixed-valence monocation of compound I. No details of the synthesis were given except to indicate that a benzene solution of iodine was used to oxidize diferrocenylacetylene. The Mössbauer spectrum of their compound, taken at 78 K, shows two quadrupole-split doublets. As can be seen in Table II, one doublet has ΔE_Q = 2.18 (2) mm/s which is close to the quadrupole splitting (ΔE_Q = 2.39 mm/s) seen for ferrocene, whereas the other doublet in the spectrum with ΔE_Q = 0.49 (2) mm/s is characteristic of an Fe(III) metallocene. It is clear that the electron-transfer rate in the mixed-valence monocation of diferrocenylacetylene is less than ca. 10^7 s^{-1}.

Figure 1 illustrates the 298-K Mössbauer spectrum of the $I_3^{-}{\cdot}^3/_4I_2$ salt of the mixed-valence monocation of compound II. Only one quadrupole-split doublet is observed, and least-squares fitting with equal-area components for the doublet gives ΔE_Q = 1.519 (5) mm/s and δ = 0.444 (7) mm/s vs. iron metal. Motoyama et al.[6] also prepared a salt of this same mixed-valence ion. The counterion for their salt was $I_3^-{\cdot}I_2$, and they reported a single quadrupole-split doublet with ΔE_Q = 1.61 (2) mm/s at 78 K. In contrast to the observation for the mixed-valence ion of compound I, the mixed-valence ion of compound II is delocalized on the ^{57}Fe Mössbauer time scale as a triiodide salt.

Magnetic Susceptibilities. Variable-temperature magnetic susceptibility data were only collected from 55.9 to 4.2 K for $[Fe(\eta^{10}\text{-}C_5H_4C{\equiv}CC_5H_4)_2Fe]I_3{\cdot}^3/_4I_2$ because of a limited sample size. The data are given in Table III, where it is seen that the effective magnetic moment per molecule varies from 2.34 μ_B at 55.9 K to 2.07 μ_B at 4.2 K. As expected, it is clear that there is one unpaired electron in the binuclear mixed-valence cation.

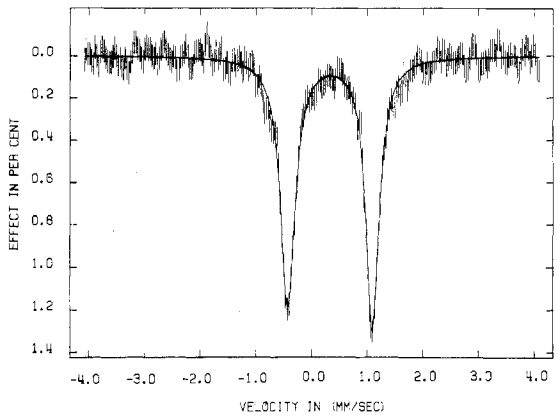

Figure 1. Room-temperature ^{57}Fe Mössbauer spectrum for $[Fe(\eta^{10}\text{-}C_5H_4C{\equiv}CC_5H_4)_2Fe]I_3{\cdot}^3/_4I_2$. The velocity scale is referenced to iron metal.

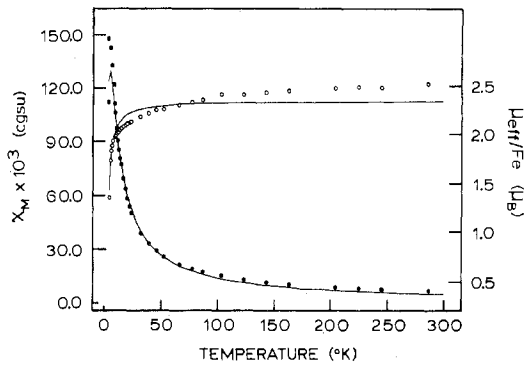

Figure 2. Experimental molar paramagnetic susceptibility (●) and effective magnetic moment per iron ion (○) vs. temperature for $[(\eta^5\text{-}C_5H_5)Fe(\eta^{10}\text{-}C_5H_4C{\equiv}CC_5H_4)Fe(\eta^5\text{-}C_5H_5)](I_3)_2$. The solid lines represent the least-squares fit to the Bleaney–Bowers equation.

Magnetic susceptibility data were measured for $[(\eta^5\text{-}C_5H_5)Fe(\eta^{10}\text{-}C_5H_4C{\equiv}CC_5H_4)Fe(\eta^5\text{-}C_5H_5)](I_3)_2$ in the range 286–4.2 K. The molar paramagnetic susceptibility (χ_M) vs. temperature and effective magnetic moment per iron ion (μ_{eff}/Fe) vs. temperature curves are presented in Figure 2, and the data are given in Table IV. There is a gradual decrease

Table IV. Corrected Paramagnetic Susceptibility Data for $[(\eta^5\text{-}C_5H_5)Fe(\eta^{10}\text{-}C_5H_4C{\equiv}CC_5H_4)Fe(\eta^5\text{-}C_5H_5)](I_3)_2$

	$10^3\chi_M$,[a] cgsu		μ_{eff}/Fe, μ_B			$10^3\chi_M$,[a] cgsu		μ_{eff}/Fe, μ_B	
T, K	exptl	calcd	exptl	calcd	T, K	exptl	calcd	exptl	calcd
286.0	5.58	4.87	2.52	2.36	21.4	52.7	57.9	2.12	2.23
245.0	6.63	5.68	2.49	2.36	19.4	57.5	62.9	2.11	2.21
224.0	6.92	6.19	2.49	2.36	17.7	62.2	67.9	2.10	2.19
204.0	7.55	6.80	2.48	2.35	15.9	68.2	74.0	2.08	2.17
163.0	9.24	8.49	2.45	2.35	14.0	76.0	81.6	2.06	2.14
143.0	10.4	9.67	2.43	2.35	13.2	79.4	85.2	2.05	2.12
122.0	11.8	11.2	2.41	2.34	12.3	84.2	89.7	2.03	2.10
103.0	14.2	13.3	2.42	2.34	11.4	89.4	94.4	2.02	2.07
86.1	16.1	15.8	2.35	2.34	10.5	96.4	99.6	2.01	2.04
76.9	17.7	17.7	2.33	2.33	9.5	105.0	105.6	2.00	2.00
65.7	20.2	20.6	2.30	2.32	8.8	110.4	110.0	1.97	1.97
52.0	24.5	25.7	2.26	2.31	7.7	121.7	116.8	1.94	1.90
45.5	27.9	29.2	2.25	2.30	6.8	131.7	121.7	1.89	1.82
38.6	32.0	34.1	2.22	2.29	5.8	145.2	124.8	1.84	1.70
31.4	37.9	41.2	2.18	2.27	5.1	147.6	123.8	1.74	1.59
23.1	49.3	54.2	2.13	2.24	4.2	109.8	115.1	1.36	1.39

[a] Molar paramagnetic susceptibilities are corrected for background and compound diamagnetism, which is calculated from Pascal's constants to be -417.1 cgsu/mol. Least-squares-fitting parameters are $J = -3.1$ cm^{-1} and $g = 2.73$.

in μ_{eff}/Fe from 2.52 μ_B at 286 K to 2.14 μ_B at 14.0 K, whereupon the μ_{eff}/Fe decreases more rapidly with decreasing temperature to a value of 1.39 μ_B at 4.2 K. The susceptibility vs. temperature data show a maximum at ca. 5 K. The magnitude of decrease in μ_{eff}/Fe at low temperatures is not characteristic of a ferrocenium system.[17] For example, μ_{eff}/Fe for $[Fe(\eta^5\text{-}C_5H_5)_2]I_3$ is 2.54 μ_B at 296 K and drops to 2.40 μ_B at 12.2 K, followed by a drop to 1.95 μ_B at 4.2 K. It appears that there is an antiferromagnetic exchange interaction present in $[(\eta^5\text{-}C_5H_5)Fe(\eta^{10}\text{-}C_5H_4C{\equiv}CC_5H_4)Fe(\eta^5\text{-}C_5H_5)](I_3)_2$.

If it is assumed that the antiferromagnetic exchange interaction present in the I_3^- salt of dioxidized diferrocenylacetylene is an intramolecular interaction within the binuclear dication, the Bleaney–Bowers susceptibility equation[18] could be used to fit the data. This equation assumes that the magnetic exchange interaction between the two $S_1 = S_2 = {}^1/_2$ centers is isotropic; that is, the spin Hamiltonian $\hat{H} = -2J\hat{S}_1\cdot\hat{S}_2$ applies. Least-squares fitting the data to the Bleaney–Bowers equation gives $J = -3.1$ cm^{-1} and $g = 2.73$. The solid lines in Figure 2 represent this fit. It is clear that the fit is poor. The gradual decrease in μ_{eff}/Fe as the sample temperature is decreased from 286 to ca. 50 K is not reproduced. This is to be expected, for the electronic ground state of the ferrocenium ion is the orbitally degenerate $^2E_{2g}$ state from the $a_{1g}{}^2\ e_{2g}{}^3$ configuration (D_{5d} symmetry labels).[19,20] The orbital angular momentum present in the $^2E_{2g}$ ground state is not accounted for with the Bleaney–Bowers equation. In spite of the poor fit, the theoretical fit does give an order of magnitude estimate of the exchange parameter J.

This is the first reporting of a magnetic exchange type of interaction for any ferrocenium or dioxidized biferrocene species. Several dioxidized bridged-ferrocenes have been examined,[17] and no indications of an exchange interaction were found. On the other hand, two dioxidized ferrocenophane-like species have been reported to be *diamagnetic*: the dication of bis(fulvalene)diiron (III)[4,17,21] and the dication of 1,12-dimethyl[1.1]ferrocenophane (IV).[4]

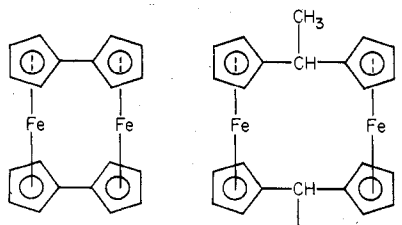

III

IV

Obviously, the X-ray structure of $[(\eta^5\text{-}C_5H_5)Fe(\eta^{10}\text{-}C_5H_4C{\equiv}CC_5H_4)Fe(\eta^5\text{-}C_5H_5)](I_3)_2$ is needed to ascertain the origin of the weak antiferromagnetic exchange interaction. There are three general possibilities. A triiodide ion could be bridging in some manner between the two $S = {}^1/_2$ iron ions in the binuclear dication. A triiodide ion could also conceivably be bridging between iron ions in two nearby dications in the lattice. These two possibilities do not seem to be too likely. The X-ray structure[22] of $[Fe(\eta^5\text{-}C_5H_5)_2]I_3$ shows discrete noninteracting $Fe(\eta^5\text{-}C_5H_5)_2{}^+$ and I_3^- ions. We recently reported[23] the structure of the triiodide salt of the mixed-valence diferrocenylselenide ion, $\{[Fe(\eta^5\text{-}C_5H_5)(\eta^5\text{-}C_5H_4)]_2Se\}I_3\cdot I_2\cdot {}^1/_2CH_2Cl_2$. Discrete mixed-valence $[Fe(\eta^5\text{-}C_5H_5)(\eta^5\text{-}C_5H_4)]_2Se^+$ cations and an anion structure consisting of zigzag chains of triiodide anions and iodine molecules are present. The acetylene moiety acting as a superexchange pathway forms the third possible mechanism of exchange in the dioxidized diferrocenylacetylene compound. This seems to be the most likely possibility.

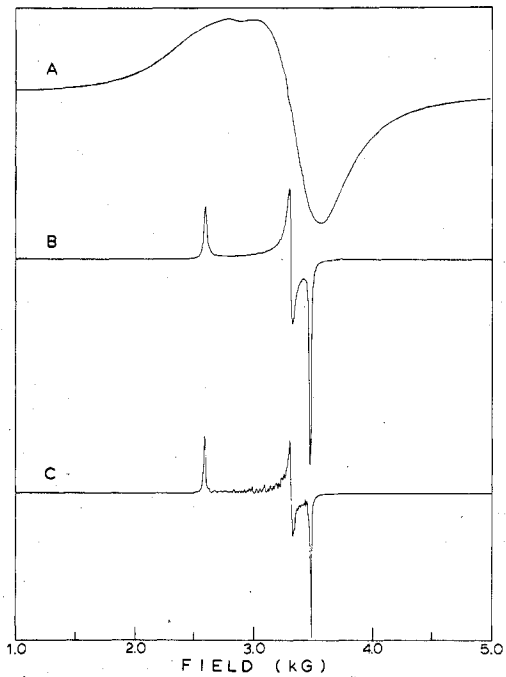

Figure 3. X-Band EPR spectra of a powdered sample of $[Fe(\eta^{10}\text{-}C_5H_4C{\equiv}CC_5H_4)_2Fe]I_3\cdot{}^3/_4I_2$ at 298 K (A), 77 K (B), and 5 K (C).

Table V. EPR Observables[a]

compd	T, K	g_1	g_2	g_3
$[Fe(\eta^{10}\text{-}C_5H_4\text{-}C{\equiv}C\text{-}C_5H_4)_2Fe]I_3\cdot{}^3/_4I_2$	298[b]	2.60	1.97	1.88
	298[c]	2.64	1.97	
	77[b]	2.59	1.98	1.88
	77[c]	2.52	1.97	1.88
	5.1[c]	2.52	1.97	1.88
$[(\eta^5\text{-}C_5H_5)Fe(\eta^{10}\text{-}C_5H_4\text{-}C{\equiv}C\text{-}C_5H_4)\text{-}Fe(\eta^5\text{-}C_5H_5)](I_3)_2$	77[c]	3.2		<1.8
	20[c]	2.33	2.13[d]	1.92
$[Fe(\eta^{10}\text{-}C_{10}H_8)_2Fe]I_3\cdot I_2$[e]	298	2.33	1.99	
	77	2.34	1.99	1.88
	12	2.36	1.99	1.91
$[(\eta^5\text{-}IC_5H_4)Fe(\eta^{10}\text{-}C_{10}H_8)\text{-}Fe(\eta^5\text{-}IC_5H_4)]I_3$[e]	77	2.79	2.02	
	12	2.75	2.01	1.97
$[(\eta^5\text{-}C_5H_5)Fe(\eta^{10}\text{-}C_{10}H_8)\text{-}Fe(\eta^5\text{-}C_5H_5)]I_3$[e]	12	3.58	1.72	
$[Fe(\eta^{10}\text{-}C_5H_4\text{-}CH(CH_3)\text{-}C_5H_4)_2Fe]I_3$[e]	12	4.28	2.07	2.03
$[(\eta^5\text{-}C_5H_5)_2Fe]I_3$[f]	20	3.67	1.77	

[a] Powdered samples. g_2 and g_3 are the perpendicular signals which when unsplit are listed as g_2. [b] Q-Band data. [c] X-Band data. [d] Additional signal at $g = 2.17$. [e] From ref 4. [f] Anderson, S. E.; Rai, R. *Chem. Phys.* 1973, *2*, 216.

Electron Paramagnetic Resonance. It was important to get EPR data for the same salt of the mixed-valence monocation of [2.2]ferrocenocenophane-1,13-diyne as had been studied by ^{57}Fe Mössbauer spectroscopy to further characterize the rate of electron transfer in this species. The $I_3^-\cdot{}^3/_4I_2$ salt was powdered, and X-band spectra were recorded at 298, 77, and 5 K. Figure 3 illustrates the data which are also summarized in Table V together with relevant data. A poorly resolved signal is seen at room temperature, whereas cooling the sample to only 77 K produces a well-resolved spectrum with g values

(17) Morrison, W. H., Jr.; Krogsrud, S.; Hendrickson, D. N. *Inorg. Chem.* **1973**, *12*, 1998.
(18) Bleaney, B.; Bowers, K. D. *Proc. R. Soc. London, Ser. A* **1952**, *214*, 451.
(19) Hendrickson, D. N.; Sohn, Y. S.; Gray, H. B. *Inorg. Chem.* **1971**, *10*, 1559.
(20) Duggan, D. M.; Hendrickson, D. N. *Inorg. Chem.* **1975**, *14*, 955.
(21) Morrison, W. H., Jr.; Hendrickson, D. N. *Inorg. Chem.* **1974**, *13*, 2279.
(22) Bernstein, T.; Herbstein, F. H. *Acta Crystallogr., Sect. B* **1968**, *B24*, 1640.
(23) Kramer, J. A.; Herbstein, F. H.; Hendrickson, D. N. *J. Am. Chem. Soc.* **1980**, *102*, 2293.

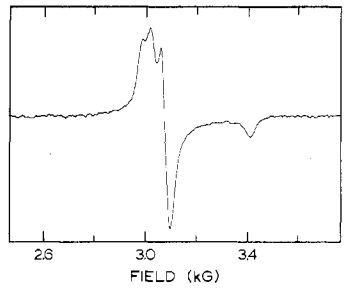

Figure 4. X-Band EPR spectrum of a powdered sample of $[(\eta^5\text{-}C_5H_5)Fe(\eta^{10}\text{-}C_5H_4C{\equiv}CC_5H_4)Fe(\eta^5\text{-}C_5H_5)](I_3)_2$ at 20 K.

of 2.52, 1.97, and 1.88. The Q-band spectrum shows a rhombic spectrum even at 298 K with g values of 2.60, 1.97, and 1.88.

The EPR signature observed for the mixed-valence monocation of the diyne compound II is very similar to those seen for the mixed-valence ions from bis(fulvalene)diiron and 1′,6′-diiodobiferrocene. Both of these latter species are believed[4,5] to be delocalized on the EPR time scale. Thus, it may be concluded that the mixed-valence monocation of compound II has an electron-transfer rate in excess of ca. 10^{10} s^{-1}.

The X-band EPR data for $[(\eta^5\text{-}C_5H_5)Fe(\eta^{10}\text{-}C_5H_4C{\equiv}CC_5H_4)Fe(\eta^5\text{-}C_5H_5)](I_3)_2$ present somewhat of a puzzlement. At 77 K the spectrum for a powdered sample consists of very broad features at g values of ca. 3.2 and 1.8. Dramatic changes in the spectrum occur when the sample is cooled to 20 K, as can be seen in Figure 4. Signals are seen at g values of 2.33, 2.17, 2.13, and 1.92. It is difficult to offer a detailed explanation for this spectrum. The presence of a weak antiferromagnetic exchange interaction in this compound could account for the spectrum. The magnetic exchange interaction between the two $S = {}^1/_2$ Fe(III) centers in this binuclear complex would exchange average the **g** tensors on the two separate iron ions to give one **g** tensor for the triplet state of the binuclear complex. Dipolar zero-field splitting could also be present which would account for the presence of more than three features.

Infrared Spectroscopy. The mixed-valence monocation of [2.2]ferrocenophane-1,13-diyne is delocalized on the ^{57}Fe Mössbauer and EPR time scales. Molecular vibrations occur on the time scale of ca. 10^{-11} s, and, consequently, it is possible to tell whether the electron-transfer rate is greater than 10^{12}–10^{13} s^{-1}. If the IR bands for a given mixed-valence monocation occur at a frequency intermediate between those for the corresponding unoxidized and dioxidized species, then it can be concluded that the monocation is delocalized. There is probably no barrier to thermal electron transfer.

The major bands[20,24] in the IR spectrum of ferrocene are found at 475, 491, 815, 1005, 1111, 1412, and 3085 cm^{-1}. The first two bands are due to ring–metal–ring stretch and tilt vibrations. The 1111-cm^{-1} band is due to the asymmetric ring-breathing vibration, and the 1412-cm^{-1} band is due to the asymmetric C–C stretch. The C–H stretch band is found at 3085 cm^{-1}. When ferrocene is oxidized to give a ferrocenium salt, ring–metal–ring stretch and tilt bands are greatly reduced in intensity.[20] Other bands show reductions in intensity which are not so pronounced. The perpendicular C–H bend, which is seen at 815 cm^{-1} for ferrocene, appears to be the most

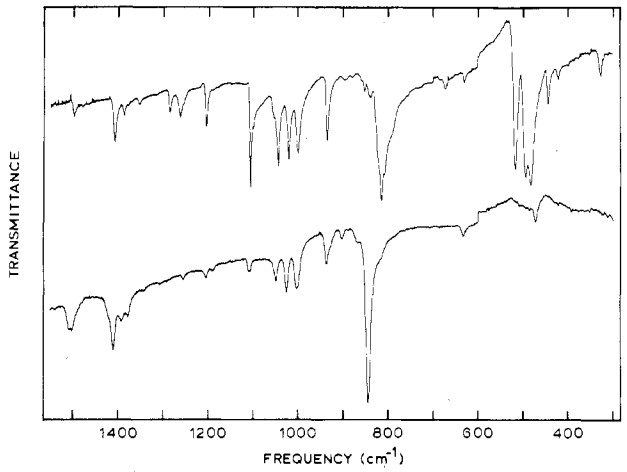

Figure 5. Infrared spectra of room-temperature KBr pellets of $(\eta^5\text{-}C_5H_5)Fe(\eta^{10}\text{-}C_5H_4C{\equiv}CC_5H_4)Fe(\eta^5\text{-}C_5H_5)$ (top) and $[(\eta^5\text{-}C_5H_5)Fe(\eta^{10}\text{-}C_5H_4C{\equiv}CC_5H_4)Fe(\eta^5\text{-}C_5H_5)](I_3)_2$ (bottom) in the region of 300–1550 cm^{-1}.

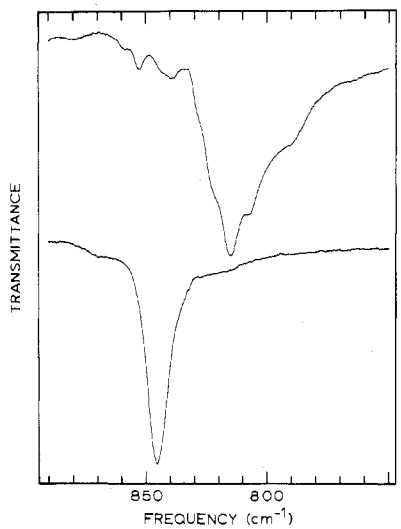

Figure 6. Expanded view of the 750–890-cm^{-1} perpendicular C–H bending region of the KBr-pellet infrared spectra of $(\eta^5\text{-}C_5H_5)Fe(\eta^{10}\text{-}C_5H_4C{\equiv}CC_5H_4)Fe(\eta^5\text{-}C_5H_5)$ (top) and $[(\eta^5\text{-}C_5H_5)Fe(\eta^{10}\text{-}C_5H_4C{\equiv}CC_5H_4)Fe(\eta^5\text{-}C_5H_5)](I_3)_2$ (bottom).

diagnostic of the oxidation state of a ferrocene. This band is found at 851 cm^{-1}, for example, for ferrocenium triiodide, and it has not lost much relative intensity in going from ferrocene to this ferrocenium salt.

The infrared spectra of diferrocenylacetylene and the I_3^- salt of the *dication* of diferrocenylacetylene are presented in Figure 5; Table VI[25] summarizes the data. Each compound was run as a KBr pellet. There is a decrease in the number and intensities of the bands in the spectrum of the dioxidized compound relative to those seen in the spectrum of diferrocenylacetylene. Figure 6 shows an expanded view of the region where the perpendicular C–H bend is found. The upper tracing for the unoxidized molecule shows a strong structured band at 815 cm^{-1}. Only a single strong band at 845 cm^{-1} is seen in the lower tracing for the I_3^- salt of the dioxidized species. Both iron ions are oxidized, and the band shifts to a value appropriate for a ferrocenium salt.

Mixed-valence triiodide salts of biferrocene and 1′-acetylbiferrocene were prepared and examined with IR spectroscopy to further check the application of IR to these compounds. The

(24) Fritz, H. P. *Adv. Organomet. Chem.* **1964**, *1*, 267. Lippincott, E. R.; Nelson, R. S. *Spectrochim. Acta* **1958**, *10*, 307. Long, T. V., Jr.; Huege, F. R. *Chem. Commun.* **1968**, 1239. Hartley, D.; Ware, M. J. *J. Chem. Soc. A* **1969**, 138. Bodenheimer, J.; Loewenthal, E.; Low, W. *Chem. Phys. Lett.* **1969**, *3*, 715. Brunvoll, J.; Cyvin, S. J.; Schafer, L. *J. Organomet. Chem.* **1971**, *27*, 107. Hyams, I. J. *Spectrochim. Acta, Part A* **1973**, *29A*, 839; *Chem. Phys. Lett.* **1973**, *18*, 399. Pavlik, I.; Klickorka, J. *Collect. Czech. Chem. Commun.* **1965**, *30*, 664. Sohar, P.; Kuszmann, J. *J. Mol. Struct.* **1969**; *3*, 359. Bailey, R. T.; Lippincott, E. R. *Spectrochim. Acta* **1965**, *21*, 389.

(25) Supplementary material.

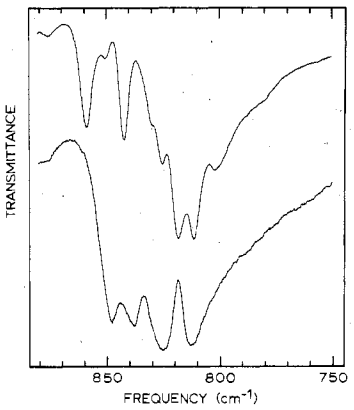

Figure 7. Perpendicular C–H bending region of the KBr-pellet infrared spectra of biferrocene (top) and biferrocenium triiodide–hemi(diiodine) (bottom).

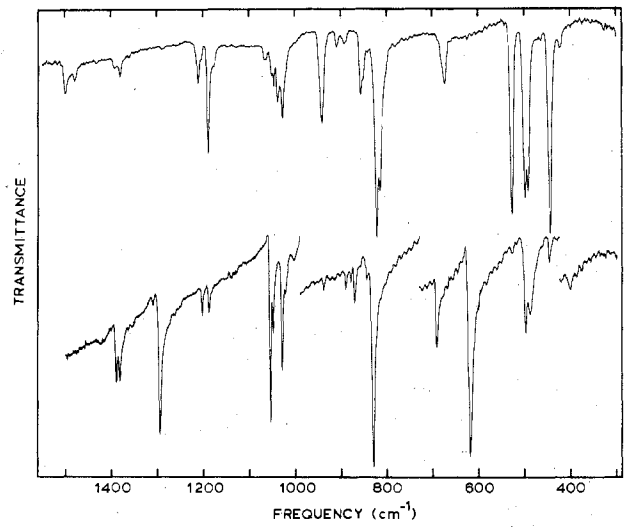

Figure 8. Infrared spectra of KBr pellets of $Fe(\eta^{10}\text{-}C_5H_4C{\equiv}CC_5H_4)_2Fe$ (top) and $[Fe(\eta^{10}\text{-}C_5H_4C{\equiv}CC_5H_4)_2Fe]I_3{\cdot}^3/_4I_2$ (bottom) in the 300–1550-cm^{-1} region.

mixed-valence biferrocene triiodide salt is known[4] to be localized on the Mössbauer time scale. The substitution of a single acetyl group on the mixed-valence biferrocene ion would be expected to enhance the localization. In fact, a Mössbauer spectrum run at room temperature for $[(\eta^5\text{-}CH_3COC_5H_4)Fe(\eta^{10}\text{-}C_{10}H_8)Fe(\eta^5\text{-}C_5H_5)]I_3{\cdot}^1/_2I_2$ does show two equal-area quadrupole-split doublets. Table II should be consulted for the data. The perpendicular C–H bending region of biferrocene and its mixed-valence triiodide salt are shown in Figure 7. The complexity of the spectrum in this region is such that a definite one-to-one relationship between the bands of the unoxidized and mixed-valence compounds is difficult to establish. It does appear, however, that bands are present in the spectrum of the mixed-valence salt that are attributable to both the Fe(II) and Fe(III) parts of the mixed-valence ion.

This is also the case for the 1′-acetylbiferrocene compounds. The unoxidized compound shows a strong band at 815 cm^{-1}. This band seems to be present as a shoulder in the spectrum of the mixed-valence salt, which also shows strong bands at 832 and 847 cm^{-1}. These latter two bands are attributable to the Fe(III) part of the mixed-valence ion.

The KBr-pellet IR spectra for [2.2]ferrocenophane-1,13-diyne and its $I_3{\cdot}^3/_4I_2$ salt are shown in Figure 8, and the band positions are given in Table VII.[25] Again there is a reduction in intensity of the bands in the 500-cm^{-1} region in going from the unoxidized compound to the mixed-valence species. The perpendicular C–H bands remain strong. An expanded view of these latter bands is shown in Figure 9, where it can be seen that only a single major absorption occurs at 830 cm^{-1} in this region for the mixed-valence ion. The position of this 830-cm^{-1} band is halfway between the analogous bands for unoxidized and dioxidized diferrocenylacetylene. It appears that the "mixed-valence" $I_3{\cdot}^3/_4I_2$ salt of [2.2]ferrocenophane-1,13-diyne is delocalized on the IR time scale.

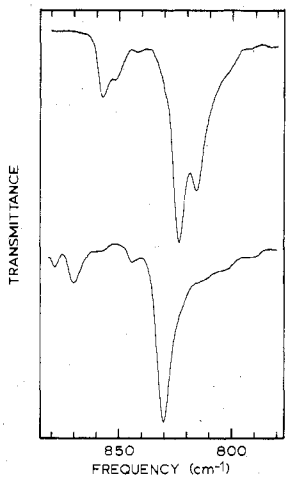

Figure 9. Perpendicular C–H bending region of the KBr-pellet infrared spectra of $Fe(\eta^{10}\text{-}C_5H_4C{\equiv}CC_5H_4)_2Fe$ (top) and $[Fe(\eta^{10}\text{-}C_5H_4C{\equiv}CC_5H_4)_2Fe]I_3{\cdot}^3/_4I_2$ (bottom).

There is yet one further interesting aspect of the IR spectrum of the $I_3{\cdot}^3/_4I_2$ salt of [2.2]ferrocenophane-1,13-diyne that should be noted (see Figure 8). Either there is a "new" band at 619 cm^{-1} or the 525-cm^{-1} band for the unoxidized compound has shifted to 619 cm^{-1}. In a previous paper,[4] we compared the IR spectra of bis(fulvalene)diiron, [bis(fulvalene)diiron]PF_6, and [bis(fulvalene)diiron]$(PF_6)_2$. An unexplained intense band at 674 cm^{-1} was observed for the mixed-valence compound. No appreciable-intensity band was seen in this region for either the unoxidized or dioxidized bis(fulvalene)diiron species. The monocation is believed to be totally delocalized.[4,5]

The mixed-valence ion resultant from oxidation of bis(fulvalene)dicobalt is also believed to be delocalized. Infrared spectra were obtained for samples of [bis(fulvalene)dicobalt]PF_6 and [bis(fulvalene)dicobalt]PF_6, as illustrated in Figure 10. The perpendicular C–H bending vibrations are, of course, masked by very strong PF_6^- bands in these spectra. It is interesting to note that again the formally mixed-valence species has a strong band at 669 cm^{-1}, where there is no band seen for the dioxidized species. At this time, an explanation for this unusual IR band is not at hand. However, it must be noted that the bis(fulvalene)dicobalt(1+) ion is clearly delocalized. This can be dramatically demonstrated by examining the Q-band EPR spectrum of a 1:1 DMF/$CHCl_3$ liquid-nitrogen-temperature glass of the PF_6^- salt. The spectrum, which is illustrated in Figure 11, shows a rhombic signal with g values of 2.21, 2.03, and 1.94. The signal at $g = 2.21$ is split into 15 hyperfine lines with a cobalt hyperfine ($I = {}^7/_2$) interaction of 72×10^{-4} cm^{-1}. The presence of 15 hyperfine lines demonstrates that this species is delocalized on the EPR time scale.

Comparison with Other Mixed-Valence Ferrocenes. A very recent communication[26] reports the results of a magnetic Mössbauer study of biferrocene, and salts of biferrocene(1+), biferrocene(2+), and ferrocenium ion. It was concluded that the iron ions in biferrocene are very similar to that in ferrocene

(26) Rudie, A. W.; Davison, A.; Frankel, R. B. *J. Am. Chem. Soc.* **1979**, *101*, 1629.

Table VIII. Mössbauer and EPR Parameters of Ferrocenium Systems Used in Δg-ΔE_Q Correlation[a]

compd	point	$\Delta E_Q(Fe^{3+})$, mm/s	T, K	Δg	T, K
$[Fe(\eta^{10}\text{-}C_{10}H_8)_2Fe]I_3 \cdot I_2$[b]	A	1.756 (2)	4.2	0.40	77
$[Fe(\eta^{10}\text{-}C_5H_4C{\equiv}CC_5H_4)_2Fe]I_3 \cdot {}^3/_4I_2$[c]	B	1.519 (5)	298	0.64	298
$[(\eta^5\text{-}IC_5H_4)Fe(\eta^{10}\text{-}C_{10}H_8)Fe(\eta^5\text{-}IC_5H_4)]I_3$[b]	C	1.388 (2)	4.2	0.76	12
$[(\eta^5\text{-}C_5H_5)Fe(\eta^{10}\text{-}C_5H_4\text{-}Se\text{-}C_5H_4)Fe(\eta^5\text{-}C_5H_5)]I_3 \cdot I_2$[c]	D	0.491 (5)	90	1.53	77
$[(\eta^5\text{-}C_5H_5)Fe(\eta^{10}\text{-}C_{10}H_8)Fe(\eta^5\text{-}C_5H_5)]I_3$[b]	E	0.381 (3)	4.2	1.86	12
$[(\eta^5\text{-}CH_3COC_5H_4)Fe(\eta^{10}\text{-}C_{10}H_8)Fe(\eta^5\text{-}C_5H_5)]I_3 \cdot {}^1/_2I_2$[c]	F	0.280 (18)	300	1.90[d]	20
$[(\eta^5\text{-}CH_3COC_5H_4)Fe(\eta^5\text{-}C_5H_5)]I_3 \cdot I_2$[c]	G	0.233 (16)[c]	300	1.86[d]	20
$[(\eta^5\text{-}C_5H_5)_2Fe]I_3$	H	0.00[e]	77	1.90[f]	20

[a] All data are for powdered samples except as noted. [b] Reference 4. [c] This work. [d] Prins, R. *Mol. Phys.* 1970, *19*, 603 (measured in glass). [e] Reference 6. [f] Anderson, S. E.; Rai, R. *Chem. Phys.* 1973, *2*, 216.

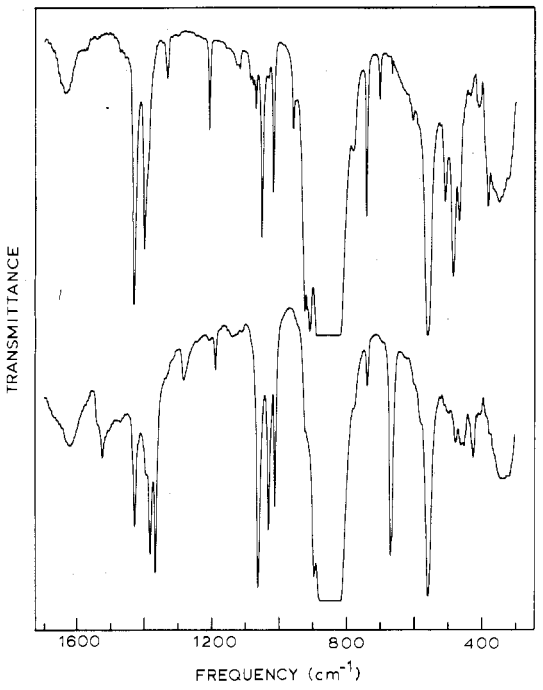

Figure 10. Infrared spectra of KBr pellets of $[Co(\eta^{10}\text{-}C_5H_4C{\equiv}CC_5H_4)_2Co](PF_6)_2$ (top) and mixed-valence $[Co(\eta^{10}\text{-}C_5H_4C{\equiv}CC_5H_4)_2Co]PF_6$ (bottom).

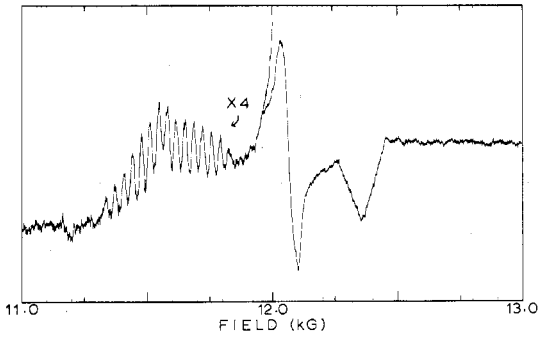

Figure 11. Q-Band EPR spectrum of $[Co(\eta^{10}\text{-}C_5H_4C{\equiv}CC_5H_4)_2Co](PF_6)$ in a 1:1 DMF/$CHCl_3$ glass at ca. 80 K.

and that those in biferrocene(2+) are the same as that in the ferrocenium ion. Interestingly, it was also concluded that the single unpaired electron in biferrocene(1+) occupies a predominantly ligand-based orbital (i.e., π-electron system of the fulvalene ligand) which is asymmetric with respect to the two iron sites. This view of the electronic structure of mixed-valence biferrocene(1+) ion struck us as being overly simplified. The description is tantamount to saying that biferrocene(1+) is in essence a mixed-valence organic species. One can only wonder how such an organic species would develop the large **g**-tensor anisotropy that has been reported[4] for salts of biferrocene(1+). A powdered sample of the triiodide salt of

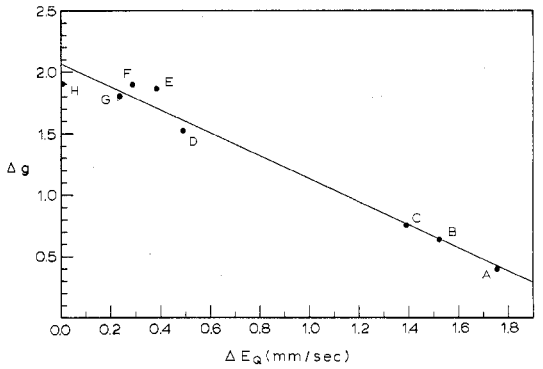

Figure 12. Plot of **g**-tensor anisotropy, $\Delta g = g_{\parallel} - g_{\perp}$, vs. quadrupole splitting, ΔE_Q, for the EPR-active part of a series of mixed-valence bridged ferrocenes. Table VIII gives the compound code and the data used in the figure.

biferrocene(1+) maintained at 12 K shows $g_{\parallel} = 3.58$ and $g_{\perp} = 1.72$, which should be a record for an organic radical.

Even the EPR delocalized mixed-valence bridged ferrocenes exhibit a **g**-tensor anisotropy that precludes describing them simply as organic radicals. The I_3^- salt of bis(fulvalene)diiron(1+) has $g_{\parallel} = 2.33$ and $g_{\perp} = 1.99$. For that matter, it can be recalled from above that the bis(fulvalene)dicobalt(1+) ion gives a spectrum with approximately the same **g**-tensor anisotropy. Indeed, the magnitude of cobalt hyperfine splitting seen is very close to that seen for cobaltocene.[27] This suggests that the orbital in which the single unpaired electron resides is predominantly metal in origin.

A comparison of the EPR properties of bis(fulvalene)diiron(1+) with those of [2.2]ferrocenophane-1,13-diyne(1+) shows that the latter ion has an appreciably larger **g**-tensor anisotropy. The EPR-delocalized 1′,6′-diiodobiferrocene(1+) ion has a larger **g**-tensor anisotropy than either of the other two EPR-delocalized ions. We have found, in fact, that there is a linear correlation between the **g**-tensor anisotropy ($\Delta g = g_{\parallel} - g_{\perp}$) and the quadrupole splitting (ΔE_Q) seen in the Mössbauer spectrum. It was further found that data for other mixed-valence bridged ferrocenes that are not delocalized on the EPR time scale could be included in the correlation. For a species that is localized on both the EPR and Mössbauer time scale, the Δg value is taken simply from the EPR spectrum, whereas the ΔE_Q value is taken as the quadrupole splitting seen for the Fe(III) doublet. Table VIII lists the values of Δg and ΔE_Q used, and Figure 12 shows the success of the correlation.

It can be seen that, starting with ferrocenium triiodide where there is essentially no quadrupole splitting and the largest $\Delta g = 0.90$, the **g**-tensor anisotropy decreases with increasing ΔE_Q until we reach the bis(fulvalene)diiron(1+) ion where the **g**-tensor anisotropy is the smallest and the single quadrupole-split doublet in the Mössbauer spectrum has $\Delta E_Q = 1.756$

(27) Ammeter, J. H.; Swalen, J. D. *J. Chem. Phys.* **1972**, *57*, 678.

(2) mm/s. The data can be fit by the least-squares method to a straight line: The coefficient of determination r^2 is 0.977. It should be noted that the ΔE_Q value used for ferrocenium triiodide is, obviously, the minimum that could be selected for this ion, as ΔE_Q values of less than ca. 0.15 mm/s are difficult to resolve. The actual point for ferrocenium triiodide will therefore be closer to the line than indicated.

The correlation of Δg with ΔE_Q suggests a continuous change in the properties of such mixed-valence bridged ferrocenes as the systems change from a localized to a delocalized moiety. In the PKS vibronic-coupling model[28] for mixed-valence compounds, three parameters are needed to describe the properties of such species. Electronic coupling between the two metal centers is gauged by ϵ, whereas the vibronic coupling is gauged by the λ parameter, which is directly proportional to the difference in the equilibrium value of the a_{1g} monomer normal coordinate in the two different oxidation states which characterize the mixed-valence compound. The third parameter is W, which gauges the difference in zero-point energy between the two states of a given mixed-valence species. In our opinion it is likely that ϵ changes from one mixed-valence ferrocene to another.

Across the series, the electronic coupling between the Fe(II) and Fe(III) ions in the mixed-valence ion is increasing. For a very localized ion, the **g** tensor is very anisotropic and ΔE_Q is small as with a monomeric ferrocenium ion. An increase in ϵ leads to a slight admixture of some of the electronic properties of the Fe(II) center into those of the Fe(III) center. The mixed-valence ion is still localized, but the Fe(III) ion has an EPR spectrum with less **g**-tensor anisotropy, and a larger ΔE_Q is seen in the Mössbauer spectrum. At some point the ion becomes delocalized. It is obvious from Figure 12 that mixed-valence bridged ferrocenes are needed that bridge the gap in the correlation, that is, ions with intermediate values of the electronic coupling.

Acknowledgment. We are grateful for support from NIH Grant HL13652 and for assistance from R. Emberson with the Mössbauer data collection. The mass spectral data processing equipment was provided by NIH Grants CA 11388 and GM 16864.

Registry No. $(\eta^5\text{-}C_5H_5)Fe(\eta^{10}\text{-}C_5H_4C{\equiv}CC_5H_4)Fe(\eta^5\text{-}C_5H_5)$, 12098-14-5; $[(\eta^5\text{-}C_5H_5)Fe(\eta^{10}\text{-}C_5H_4C{\equiv}CC_5H_4)Fe(\eta^5\text{-}C_5H_5)](I_3)_2$, 73946-44-8; $[(\eta^5\text{-}C_5H_5)Fe(\eta^{10}\text{-}C_5H_4C{\equiv}CC_5H_4)Fe(\eta^5\text{-}C_5H_5)](BF_4)_2$, 74779-52-5; $[Fe(\eta^{10}\text{-}C_5H_4C{\equiv}CC_5H_4)_2Fe)]I_3$, 74779-53-6; $[(\eta^5\text{-}C_5H_5)Fe(\eta^{10}\text{-}C_{10}H_8)Fe(\eta^5\text{-}C_5H_5)]I_3$, 39470-17-2; $(\eta^5\text{-}CH_3COC_5H_4)Fe(\eta^{10}\text{-}C_{10}H_8)Fe(\eta^5\text{-}C_5H_5)$, 59197-46-5; $[(\eta^5\text{-}CH_3COC_5H_9)Fe(\eta^{10}\text{-}C_{10}H_8)Fe(\eta^5\text{-}C_5H_5)]I_3$, 74779-55-8; $[Co(\eta^{10}\text{-}C_{10}H_9)_2Co](PF_6)_2$, 39333-80-7; $[Co(\eta^{10}\text{-}C_{10}H_8)_2Co]PF_6$, 69365-59-9; $[(\eta^5\text{-}CH_3COC_5H_4)Fe(\eta^5\text{-}C_5H_5)]I_5$, 74779-56-9; $Fe(\eta^{10}\text{-}C_5H_4C{\equiv}CC_5H_4)_2Fe$, 59187-97-2; $[(\eta^5\text{-}C_5H_5)Fe(\eta^{10}\text{-}C_5H_4\text{–}Se\text{–}C_5H_4)Fe(\eta^5\text{-}C_5H_5)]I_3$, 74779-57-0; $[Co(\eta^{10}\text{-}C_5H_4C{\equiv}CC_5H_4)_2Co](PF_6)_2$, 74779-59-2; $[Co(\eta^{10}\text{-}C_5H_4C{\equiv}CC_5H_4)_2Co]PF_6$, 74792-77-1.

Supplementary Material Available: Tables VI (IR data for diferrocenylacetylene and its dioxidized I_3^- salt) and VII (IR data for [2.2]ferrocenophane-1,13-diyne and its I_3^- salt) (2 pages). Ordering information is given on any current masthead page.

(28) Wong, K. Y.; Schatz, P. N.; Piepho, S. B. *J. Am. Chem. Soc.* **1979**, *101*, 2793. Krausz, E. R.; Schatz, P. N. *Ibid.* **1978**, *100*, 2996.

Contribution from the Department of Chemistry, University of California, Berkeley, California 94720

Metal Clusters. 26.[1] Hydrogenation of Bridging Alkyne Ligands in Dinuclear Molybdenum Complexes

S. SLATER and E. L. MUETTERTIES*

Received May 30, 1980

At temperatures above 100 °C, hydrogen reacts with $(\eta^5\text{-}C_5H_5)_2Mo_2(CO)_4(RC_2R)$ to form *cis*-RCH=CHR and $(\eta^5\text{-}C_5H_5)_2Mo_2(CO)_4$. In the presence of excess alkyne, the reaction is catalytic with turnover rates of ~0.03/min at 150 °C. In the catalytic reaction, the product olefin was the cis isomer; no trans isomer was detected in the 2-butyne, 3-hexyne, and $C_2H_2(+D_2)$ reactions. Alkyne exchange between free alkyne and complexed alkyne occurred above 100 °C. At higher temperatures, additional reactions became significant, primarily acetylene insertions to form complex metallacyclic species. This competing insertion reaction was notable for reaction systems with C_2H_2 and with 2-butyne as the free or complexed ligand. Slow thermal dissociation of $(\eta^5\text{-}C_5H_5)_2Mo_2(CO)_4(C_2H_2)$ to $(\eta^5\text{-}C_5H_5)_2Mo_2(CO)_4$ and C_2H_2 was demonstrated at 150 °C; none was detected for the substituted acetylene derivatives. The new $(\eta^5\text{-}C_5H_5)_2Mo_2(CO)_3[P(OCH_3)_3](RC_2R)$ complex was prepared and shown to be a catalyst precursor for acetylene hydrogenation to cis olefins. This complex was more active than the parent complexes by at least 1 order of magnitude. Disproportionation of the complex occurred under catalytic conditions to form $(\eta^5\text{-}C_5H_5)_2Mo_2(CO)_4(RC_2R)$ and presumably $(\eta^5\text{-}C_5H_5)_2Mo_2(CO)_2[P(OCH_3)_3]_2$. To test for fragmentation in the $(\eta^5\text{-}C_5H_5)_2Mo_2(CO)_4(RC_2R)$ hydrogenation reaction and in the acetylene-exchange reaction, we used a mixture of the $(C_5H_5)_2Mo_2$ complex and the $(CH_3C_5H_4)_2Mo_2$ complex. Ligand label interchange was not detected. Thus, fragmentation is not an integral part of these reaction cycles. Carbon monoxide inhibited the hydrogenation reaction and the acetylene-interchange reaction. Exchange between ^{13}CO and the molybdenum–acetylene complexes was fast at the temperatures (110–150 °C) of the hydrogenation and acetylene-exchange reactions, but CO and the molybdenum–acetylene compounds did not form a spectroscopically detectable complex at 110 °C and 2 atm. Kinetic studies of the acetylene-exchange reaction established the rate law to be of the form $k_1[(C_5H_5)_2Mo_2(CO)_4(RC_2R)]$. For both the hydrogenation reaction and the alkyne-exchange reaction, the first step must comprise CO dissociation to give $(\eta^5\text{-}C_5H_5)_2Mo_2(CO)_3(\mu_x\text{-}RC_2R)$. In the cocompetition of CO for this intermediate, acetylenes are more effective than is hydrogen.

Introduction

Interactions of acetylenes with metal atoms in polynuclear metal complexes are complex and rarely comprise simple σ–π complex formation centered at a single metal atom in the polynuclear assembly. Illustrated in **1**–**4** are representative interactions[2] rendered in skeletal form without depiction of acetylene substituent atoms and other metal ligand atoms. Earlier, we described the reactivity of typical representatives

(1) M. Tachikawa and E. L. Muetterties, *J. Am. Chem. Soc.*, **102**, 4541 (1980).

(2) For a discussion of polynuclear metal–alkyne complexes see E. L. Muetteries, T. N. Rhodin, E. Band, C. F. Brucker, and W. R. Pretzer, *Chem. Rev.*, **79**, 91 (1979).

0020-1669/80/1319-3337$01.00/0